Order online now!

www.rockland.com
tech@rockland.com
+1 484.791.3823

Datasheet for BSA-10

Bovine Serum Albumin - Fraction V

Overview

Description:	Bovine Serum Albumin - Fraction V (Immunoglobulin and Protease Free) - BSA-10
Item No.:	BSA-10
Size:	10 g
Applications:	ELISA, FC, Functional Assay, IF, IHC, LFA, WB
Origin:	Bovine

Product Details

Background:	Bovine Serum Albumin (BSA) is used for various biochemical applications including ELISA (Enzyme-Linked Immunosorbent Assay), high content screening assays, western blotting, FACS Buffer and immunohistochemistry. BSA as a blocking reagent is particularly useful with casein-sensitive antibodies, such as phospho-specific antibodies. Also used as a nutrient in cell and microbial culture. In restriction digests, BSA is used to stabilize some enzymes during digestion of DNA and to prevent adhesion of the enzyme to reaction tubes and other vessels. Bovine Serum Albumin can also be used to determine the quantity of other proteins, by comparing an unknown quantity of protein to known amounts of BSA.
Synonyms:	Bovine serum albumin fraction V, Bovine Albumin, BSA, BSA Blocker, BSA Blocking
Species of Origin:	Bovine

Target Details

Purity/Specificity:	Purity (%): 100% by Agarose Zone electrophoresis Moisture (%) 5% Loss on Drying pH: 7.0 Ash: <2.0% Protein (%): 98% by nitrogen analysis Protease: <0.005 Units/mg Heavy Metals: (Pb) < 10 ppm by ICP Endotoxin: < 3 EU/mg by LAL IgG: Not Detected NEFA: N/A
Relevant Links:	• BSA-10 SDS

Application Details

Suggested Applications:	ELISA, FC, Functional Assay, IF, IHC, LFA, WB (Based on references)
Application Note:	Bovine Serum Albumin - Fraction V is suitable for use in lateral flow, in protease sensitive assays such as RIA, EIA and nucleic acid hybridization, use as a stabilizing agent for proteins and enzymes including dilute solutions of antibody, use as a blocking agent to reduce non-specific binding for FACS, IF, IHC, and WB.
Assay Dilutions:	All assays should be optimized by the user. Recommended dilutions (if any) may be listed below.
ELISA:	User Optimized
FC:	User Optimized
FLISA:	User Optimized
IF:	User Optimized
IHC:	User Optimized
IP:	User Optimized
WB:	User Optimized
Other:	Purity (%): 100% by Agarose Zone electrophoresis Moisture (%) 0.9 % Loss on Drying pH: 7.0 Protein (%): 100.5 % by nitrogen analysis. Protease: <0.005 Units/mg Heavy Metals: < 0.49 ppm by ICP Endotoxin: < 0.1 EU/mg by LAL

Formulation

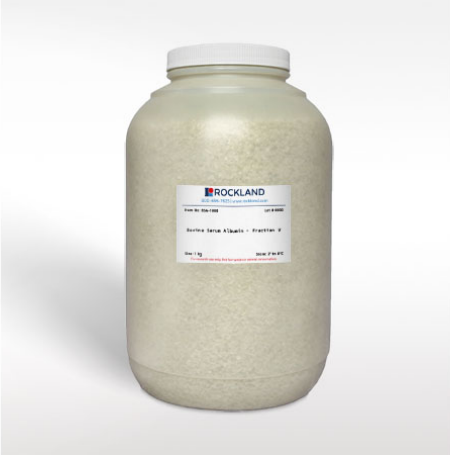
Physical State:	Lyophilized
Concentration:	N/A
Buffer:	None
Preservative:	None

Stabilizer:	None
Reconstitution Buffer:	Restore with deionized water (or equivalent)

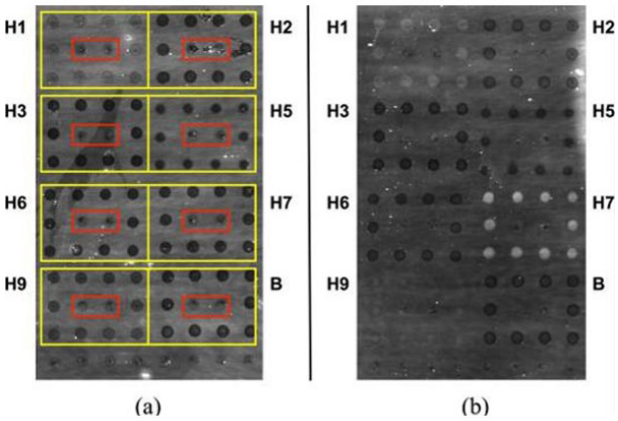
Shipping & Handling

Shipping Condition:	Ambient
Storage Condition:	Store container at 4° C prior to opening.
Expiration:	Expiration date is one (1) year from date of receipt.

Images

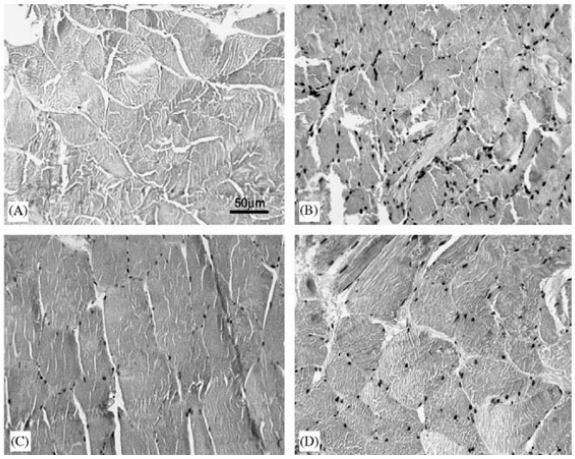


Bottle
Bovine Serum Albumin - Fraction V



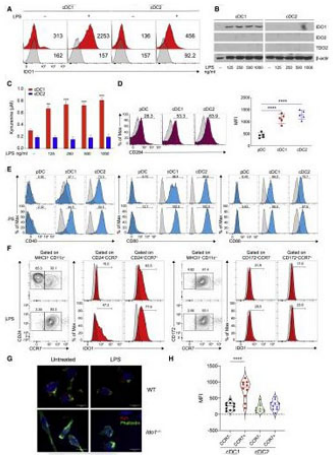
Dot Blot

Strong responses to polyclonal anti-HA antiserum are readily observable on an AIR hemagglutinin microarray.(a) 1% BSA control (p/n BSA-10). (b) Anti-H7 polyclonal antiserum (A/Netherlands/219/2003, H7N7), 1:80 dilution (1.3%) in 1% BSA. Spots showing substantially increased brightness indicate binding to immobilized H7. In both cases, antigens were arrayed in square patterns as indicated by the yellow boxes in (a); a mouse IgG Fc domain (p/n 010-0103) was included as negative control (red boxes). Slight differences in spot intensity in the control (a) are due to differences in deposition efficiency for different antigens or controls. Specific antigens used in these experiments are indicated in Table 2. Goat anti-fluorescein, (p/n 600-101-096) used as an internal negative control.
Fig 1. PMID: 26241048.



Immunohistochemistry

(I) Immunostaining for 8OhdG: (A) negative control, (B) muscle from subject 465 yr (positive control), (C) muscle from weight maintainer, and (D) muscle from weight gainer. For the 8OHdG assay, samples were treated with 10 mg/ml Proteinase K in phosphate-buffered saline (PBS) (0.05 M phosphate, 0.15 M NaCl, pH 7.4) with 1% bovine serum albumin (p/n BSA-50) for 40 min at 37 1C, and incubated in 5% skim milk in PBS for 2 h. Figure 1. PMID: 16687193.



Flow Cytometry

IDO1 is selectively induced in cDC1 cells following LPS stimulation

(A) IDO1 expression was analyzed by IS in BMDCs (n = 5).

(B) Immunoblot analysis was carried out for IDO1, IDO2, TDO2, and β-actin expression (n = 3).

(C) Supernatants from cells prepared as in (B) were analyzed for l-kynurenine content by HLPC.

(D and E) Flow plot (left) and quantification (right) of CD284 (D), and flow plot of CD40, CD80, and CD86 (E) on DC subsets (n = 3).

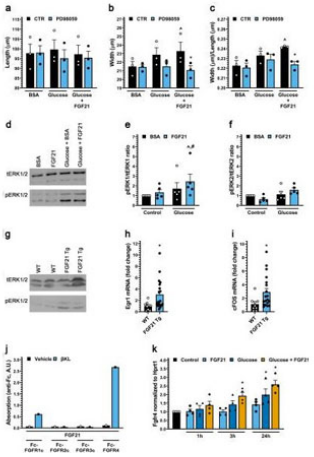
(F) BM-derived cDC1 and cDC2 were treated as in (B) and IDO1 expression evaluated in CCR7− and CCR7+ populations treated as in (B), pre-gated on cDC1 and cDC2 (n = 3).

(G) Immunofluorescence analysis of l-kynurenine expression in sorted CCR7+ cDC1 of different genotypes treated as in (B) (n = 3).

(H) IDO1 expression (MFI) in thymic CCR7− and CCR7+ dendritic cell subsets, gated on CD11c+MHCII+XCRI +CD117− and CD11c+MCHII+CD172+CD117− (n = 3).

Data are shown as mean ± SD. □□ $p < 0.01$, □□□ $p < 0.001$, □□□□ $p < 0.0001$, one-way (D and H) or two-way (C) ANOVA followed by Bonferroni multiple comparison test. Isotype control as gray histogram.

Figure 1. PMID: 35704993.



Western Blot

FGF21 activates ERK1/2 in cultured cardiac myocytes in the presence of high glucose and in heart tissue of mice. (a–c) Length, width and width to length ratio for ARVMs treated with BSA (control), FGF21 (25 ng/ml), increased glucose and/or the MEK inhibitor PD98059 (20 µM) for 48 h. Bars and colored symbols indicate average mean and means of independent experiments using different myocyte preparations, respectively. (d–f) Western blot analysis of ARVMs treated with BSA (control) or mouse recombinant FGF21 (25 ng/ml) with or without 10 mM glucose for 6 h. ERK1 is p44 and ERK2 is p42. (g) Analysis of cardiac tissue from FGF21 Tg mice and wild-type littermates at 8–12 weeks of age by Western blotting. (h, i) qRT-PCR for Egr-1 and c-Fos mRNA using total RNA from heart tissue of FGF21 Tg mice and wild-type littermates at 8–12 weeks of age. (j) Binding of 1 µg of soluble β-klotho (βKL) or PBS, 500 ng of Fc-tagged FGFR 1c, 2c, 3c, or 4 to 96-well plates coated with 200 ng of FGF21. (k) qRT-PCR for FGFR4 mRNA using total RNA isolated from ARVMs treated with BSA (control), FGF21 (25 ng/ml), and/or increased glucose (15.6 mM total). Comparison between groups was performed in form of a one-way (a–c, k) or two-way (e–f) ANOVA followed by post-hoc Tukey test or a two tailed t-test (h, i). All values are expressed as mean ± SEM. (a–c) N = 3, ^p ≤ 0.05 vs. BSA CTR, *p ≤ 0.05 vs. Glucose + FGF21 CTR; (e, f) N = 5, ^p ≤ 0.05 vs. BSA CTR, #p ≤ 0.05 vs. FGF21 CTR; (h, i) N = 9–19, *p ≤ 0.05 vs. WT; (k) N = 4, *p ≤ 0.05 vs. CTR. All Western blots are cropped, and original blots are presented in Supplementary Fig. 3. Figure 3. PMID: 35513431.

References

- Herrera-Ramirez D et al. Helicobacter pylori infection activates the HIF-1α/ALS2/Rab5 signaling axis in gastric cells. *Cell Commun Signal.* (2026)
- Ugalde V et al. Preclinical evaluation of nitrated α-synuclein-specific CAR-Treg therapy in Parkinson's disease. *Cell Rep Med.* (2026)
- Du S et al. Diversity and immune dynamics of choroid plexus macrophages are shaped by distinct developmental origins. *Nat Neurosci.* (2026)
- Butt JN et al. A multi-readout photonic sensor for rapid diagnosis of Von Willebrand disease. *NPJ Biosens.* (2026)
- Chen YC et al. Convergent Roles of Growth Differentiation Factor-15 (GDF-15) in Mechanotransduction, Vascular Disorganization, and Immune Suppression in Melanoma. *bioRxiv [Preprint].* (2026)

- Xiao Y et al A worm-like nucleic acid nanostructure for gene delivery and endosomal escape via ClC3 ion exchanger. *Sci Adv.* (2026)
- Gill SK et al. Latency-Associated Peptide Rapidly Upregulates Neuraminidase 3 in a Profibrotic Translation-Based Positive Feedback Loop. *Cells.* (2026)
- Bouzekri A et al. A Computational Workflow for Cell Line Profiling by Imaging Mass Cytometry. *Cytometry A.* (2026)
- Ohtsu A et al. Vertical-flow porous microchamber arrays for cell capture, intracellular molecule staining, and population analysis. *RSC Adv.* (2026)
- Klose AM et al. Dual-Scale StaphAIR: Predictive Modeling for the Diagnosis of S. aureus Infection via Simultaneous Detection and Quantification of Cytokines and Antibodies. *Anal Chem.* (2026)
- Johnson CF et al. RIPK3 Protects Against Endothelial Activation and Vascular Permeability in a Mouse Model of Ischemia-Reperfusion Injury. *Arterioscler Thromb Vasc Biol.* (2026)
- Khare V et al. Cystinosin regulates Na+/H+ exchanger 3 trafficking and function in kidney proximal tubular cells. *EMBO Rep.* (2026)
- Antonova AU et al. Age- and tissue-dependent diversity of human plasmacytoid dendritic cells uncovers a cycling subset dominant in early life and cancer. *Immunity.* (2026)
- Mercer TJ et al. Phosphorylated ubiquitin is a secondary messenger and an epigenetic mark mediating mitochondria to nucleus signaling. *bioRxiv [Preprint].* (2026)
- Huang RR et al. A Strategy for Simultaneous Engineering of Interspecies Cross-Reactivity, Thermostability, and Expression of a Bispecific 5T4 x CD3 DART® Molecule for Treatment of Solid Tumors. *Antibodies (Basel).* (2025)
- Fachi JL et al. Fiber- and acetate-mediated modulation of MHC-II expression on intestinal epithelium protects from Clostridioides difficile infection. *Cell Host Microbe.* (2025)
- Rodrigues PF et al. Rorγt-positive dendritic cells are required for the induction of peripheral regulatory T cells in response to oral antigens. *Cell.* (2025)
- Lee EWY et al. iNOS Mediates High-Fat Diet-Associated Aggravation of Complete Freund's Adjuvant-Induced Inflammatory Pain. *Int J Mol Sci.* (2025)
- Chung HS et al. Therapeutic potential of phytochemical luteolin in restoring skin barrier by inhibiting antimicrobial peptides associated with TRAF6/TAK1/IKK/IκB in psoriasis-like HaCaT models. *Food Sci Biotechnol.* (2025)
- Klose AM et al. Lambda Theta Reflectometry: A New Technique for Measuring Optical Film Thickness in Planar Protein Arrays. *ACS Sens.* (2025)
- Rauner G et al. Single-cell organogenesis captures complex breast tissue formation in three dimensions. *Development.* (2025)
- Launonen H et al. Ketogenic diet influences the renin-angiotensin-aldosterone system components in the healthy and inflamed intestine of male mice. *J Nutr Biochem.* (2025)
- Rossotti MM et al. A Safe and Accessible Cell-Based Spike-ACE2 Binding Assay for Evaluating SARS-CoV-2 Neutralization Activity in Biological Samples Using Flow Cytometry. *Methods Protoc.* (2025)
- Butt JN et al. A Dual-Readout Photonic Sensor for Simultaneous Measurement of Enzyme Activity and Concentration. *ACS Sens.* (2025)

- Hori A et al. Designing Porosity-Tailored Hydrogel Sponges with Controlled Cell Positioning Using Dispersible, Autofragmented Sacrificial Microfibers. *ACS Omega.* (2025)
- Saito Y et al. Enhancing cancer cell immunocapture on orientation-controlled nanoimprinted microcone arrays in microgap channels. *Lab Chip.* (2025)
- Bucukovski J et al. Everything's under Control: Maximizing Biosensor Performance through Negative Control Probe Selection. *Anal Chem.* (2025)
- Bisson JA et al. GATA6 regulates WNT and BMP programs to pattern precardiac mesoderm during the earliest stages of human cardiogenesis. *Elife.* (2025)
- Mehrotra S et al. Pharmacological Characterization of Zasocitinib (TAK-279): An Oral, Highly Selective, and Potent Allosteric TYK2 Inhibitor. *J Invest Dermatol.* (2025)
- Eshraghi J et al. Subvisible particle formation under mechanical and interfacial stress: A case study using bovine serum albumin as a model for biotherapeutic proteins. *Int J Pharm.* (2025)
- Schuster-Little N et al. Immunoaffinity-free chromatographic purification of ovarian cancer biomarker CA125 (MUC16) from blood serum enables mass spectrometry characterization. *Anal Methods.* (2024)
- Seo T et al. MARCH family E3 ubiquitin ligases selectively target and degrade cadherin family proteins. *PLoS One.* (2024)
- Walter LD et al. Transcriptomic analysis of skeletal muscle regeneration across mouse lifespan identifies altered stem cell states. *Nat Aging.* (2024)
- Jarvi NL et al. Immune regulatory adjuvant approach to mitigate subcutaneous immunogenicity of monoclonal antibodies. *Front Immunol.* (2024)
- Afshar-Saber W et al. ALDH5A1-deficient iPSC-derived excitatory and inhibitory neurons display cell type specific alterations. *Neurobiol Dis.* (2024)
- Sun Y et al. Methionine availability influences essential H3K36me3 dynamics during cell differentiation. *bioRxiv [Preprint].* (2023)
- Tian JL et al. Regulation of Primary Cilium Length by O-GlcNAc during Neuronal Development in a Human Neuron Model. *Cells.* (2023)
- Nishi K et al. IL-6-Mediated Upregulated miRNAs in Extracellular Vesicles Derived from Lund Human Mesencephalic (LUHMES) Cells: Effects on Astrocytes and Microglia. *Biomolecules.* (2023)
- Mazaki Y et al. LRRK2 is involved in the chemotaxis of neutrophils and differentiated HL-60 cells, and the inhibition of LRRK2 kinase activity increases fMLP-induced chemotactic activity. *Cell Commun Signal.* (2023)
- Helble JD et al. Single-cell RNA sequencing of murine ankle joints over time reveals distinct transcriptional changes following Borrelia burgdorferi infection. *iScience.* (2023)
- Chen W et al. The mRNA-binding protein DDX3 mediates TGF-β1 upregulation of translation and promotes pulmonary fibrosis. *JCI Insight.* (2023)
- Neira V et al. Identification and characterization of porcine Rotavirus A in Chilean swine population. *Front Vet Sci.* (2023)
- Kurosaki T et al. Integrative omics indicate FMRP sequesters mRNA from translation and deadenylation in human neuronal cells. *Mol Cell.* (2022)

- Cho H et al. AKT constitutes a signal-promoted alternative exon-junction complex that regulates nonsense-mediated mRNA decay. *Mol Cell.* (2022)
- Yang X et al. Qualitative immunoassay for the detection of anti-SARS-COV-2 spike antibody in human milk samples. *STAR Protoc.* (2022)
- Chio TI et al. A BODIPY-Based Probe Enables Fluorogenicity via Thiol-Dependent Modulation of Fluorophore Aggregation. *Molecules.* (2022)
- Pilling D et al. The sialidase NEU3 promotes pulmonary fibrosis in mice. *Respir Res.* (2022)
- Lee IK et al. Monitoring Therapeutic Response to Anti-FAP CAR T Cells Using [18F]AlF-FAPI-74. *Clin Cancer Res.* (2022)
- Kirolos SA et al. The extracellular sialidase NEU3 primes neutrophils. *J Leukoc Biol.* (2022)
- Gargaro, M et al. Indoleamine 2,3-dioxygenase 1 activation in mature cDC1 promotes tolerogenic education of inflammatory cDC2 via metabolic communication. *Immunity* (2022)
- Yanucil, C et al. FGF21-FGFR4 signaling in cardiac myocytes promotes concentric cardiac hypertrophy in mouse models of diabetes. *Scientific Reports* (2022)
- Christopher Yanucil et al. Soluble α-klotho and heparin modulate the pathologic cardiac actions of fibroblast growth factor 23 in chronic kidney disease. *Kidney Int.* (2022)
- Rahman F et al. DYNC1LI2 regulates localization of the chaperone-mediated autophagy receptor LAMP2A and improves cellular homeostasis in cystinosis. *Autophagy.* (2021)
- Papimi D et al. The Aurora B gradient sustains kinetochore stability in anaphase. *Cell Rep.* (2021)
- Woodworth MA et al. Multiplexed single-cell profiling of chromatin states at genomic loci by expansion microscopy. *Nucleic Acids Research* (2021)
- Portillo AL et al. Production of human CAR-NK cells with lentiviral vectors and functional assessment in vitro. *STAR Protoc.* (2021)
- Boccasavia, VL et al. Antigen presentation between T cells drives Th17 polarization under conditions of limiting antigen. *Cell Reports* (2021)
- Kurosaki, T et al. Loss of the fragile X syndrome protein FMRP results in misregulation of nonsense-mediated mRNA decay. *Nature Cell Biology* (2021)
- Ahn TS et al. Commercial immunoglobulin products contain cross-reactive but not neutralizing antibodies against SARS-CoV-2. *J Allergy Clin Immunol.* (2021)
- Burgos-Bravo F et al. Application of Force to a Syndecan-4 Containing Complex With Thy-1–αVβ3 Integrin Accelerates Neurite Retraction. *Front Mol Biosci.* (2020)
- Zhang J, et al. Diminution of Phagocytosed Micro/Nanoparticles by Tethering with Immunoregulatory CD200 Protein. *Sci Rep.* (2020)
- Zhang J, et al. Blockade of Macrophage Adhesion to CD200-treated Polystyrene Culture Surface. *J Biomed Mater Res A.* (2020)
- Porterfield V. et al. A three-dimensional dementia model reveals spontaneous cell cycle re-entry and a senescence-associated secretory phenotype. *Neurobiol Aging.* (2020)

- Mao C. et al. Feature-rich covalent stains for super-resolution and cleared tissue fluorescence microscopy. *Sci Adv.* (2020)
- Schuster-Little N, Madera S, Whelan R. Developing a mass spectrometry-based assay for the ovarian cancer biomarker CA125 (MUC16) using suspension trapping (STrap). *Anal Bioanal Chem.* (2020)
- Gronseth, E et al. Astrocytes influence medulloblastoma phenotypes and CD133 surface expression. *PloS One* (2020)
- Christensen SC et al. Characterization of basigin monoclonal antibodies for receptor-mediated drug delivery to the brain. *Sci Rep.* (2020)
- Ferdman J et al. Intra-seasonal antibody repertoire analysis of a subject immunized with an MF59®-adjuvanted pandemic 2009 H1N1 vaccine. *Vaccine.* (2019)
- Moreno-Olivas F et al. ZnO nanoparticles affect nutrient transport in an in vitro model of the small intestine. *Food Chem Toxicol.* (2019)
- Leung CS, Douglass SM, Morselli M, et al. H3K36 Methylation and the Chromodomain Protein Eaf3 Are Required for Proper Cotranscriptional Spliceosome Assembly. *Cell Rep.* (2019)
- Pollock SR, Schinlever AR, Rohani A, Kashatus JA, Kashatus DF. RalA and RalB relocalization to depolarized mitochondria depends on clathrin-mediated endocytosis and facilitates TBK1 activation. *PLoS One.* (2019)
- Zhang J, He J, Johnson JL, et al. Cross-regulation of defective endolysosome trafficking and enhanced autophagy through TFEB in UNC13D deficiency. *Autophagy.* (2019)
- Mondanelli G, Volpi C. Differentiation of Myeloid-derived Suppressor Cells from Murine Bone Marrow and Their Co-culture with Splenic Dendritic Cells. *Bio Protoc.* (2017)
- Allen JN, Dey A, Nissly R, et al. Isolation, Characterization, and Purification of Macrophages from Tissues Affected by Obesity-related Inflammation. *J Vis Exp.* (2017)
- Chang Q, Ornatsky O, Hedley D. Staining of Frozen and Formalin-Fixed, Paraffin-Embedded Tissues with Metal-Labeled Antibodies for Imaging Mass Cytometry Analysis. *Curr Protoc Cytom.* (2017)
- Spencer, KC et al. A three dimensional in vitro glial scar model to investigate the local strain effects from micromotion around neural implants. *Lab on a Chip* (2017)
- Raymond DD et al. Influenza immunization elicits antibodies specific for an egg-adapted vaccine strain. *Nat Med.* (2016)
- Domogauer JD, de Toledo SM, Azzam EI. A Mimic of the Tumor Microenvironment: A Simple Method for Generating Enriched Cell Populations and Investigating Intercellular Communication. *J Vis Exp.* (2016)
- Schmidt AG et al. Viral receptor-binding site antibodies with diverse germline origins. *Cell.* (2015)
- Bucukovski, J et al. A Multiplex Label-Free Approach to Avian Influenza Surveillance and Serology. *PloS One* (2015)
- Keeler, GD et al. Effects of delayed delivery of dexamethasone-21-phosphate via subcutaneous microdialysis implants on macrophage activation in rats. *Acta Biomaterialia* (2015)
- Keeler, GD et al. Localized delivery of dexamethasone-21-phosphate via microdialysis implants in rat induces M(GC) macrophage polarization and alters CCL2 concentrations. *Acta Biomaterialia* (2015)
- Toops, KA et al. A detailed three-step protocol for live imaging of intracellular traffic in polarized primary porcine RPE monolayers. *Experimental Eye Research* (2014)

- Keeler, GD et al. Comparison of microdialysis sampling perfusion fluid components on the foreign body reaction in rat subcutaneous tissue. *European Journal of Pharmaceutical Sciences : Official Journal of the European Federation for Pharmaceutical Sciences* (2014)
- Andrew O Fung et al. Quantitative detection of PfHRP2 in saliva of malaria patients in the Philippines *Malar J.* (2012)
- Clausen TM, Christoffersen S, Dahlbäck M, et al. Structural and functional insight into how the Plasmodium falciparum VAR2CSA protein mediates binding to chondroitin sulfate A in placental malaria. *J Biol Chem.* (2012)
- Lehtinen, J et al. Pre-targeting and direct immunotargeting of liposomal drug carriers to ovarian carcinoma. *PloS One* (2012)
- Dahlbäck M, Jørgensen LM, Nielsen MA, et al. The chondroitin sulfate A-binding site of the VAR2CSA protein involves multiple N-terminal domains. *J Biol Chem.* (2011)
- Lee CH, Bose S, Van Vliet KJ, Karp JM, Karnik R. Studying cell rolling trajectories on asymmetric receptor patterns. *J Vis Exp.* (2011)
- Makino N, Maeda T, Oyama J, et al. Antioxidant therapy attenuates myocardial telomerase activity reduction in superoxide dismutase-deficient mice. *J Mol Cell Cardiol.* (2011)
- Lee, Chia-Hua et al. Examining the lateral displacement of HL60 cells rolling on asymmetric P-selectin patterns. *Langmuir : the Acs Journal of Surfaces and Colloids* (2011)
- Moorjani S, Nielson R, Chang XA, Shear JB. Dynamic remodeling of subcellular chemical gradients using a multi-directional flow device. *Lab Chip.* (2010)
- Resende M, Ditlev SB, Nielsen MA, et al. Chondroitin sulphate A (CSA)-binding of single recombinant Duffy-binding-like domains is not restricted to Plasmodium falciparum Erythrocyte Membrane Protein 1 expressed by CSA-binding parasites. *Int J Parasitol.* (2009)
- Dravid G, Hammond H, Cheng L. Culture of human embryonic stem cells on human and mouse feeder cells. *Methods Mol Biol.* (2006)
- de la Maza MP, Olivares D, Hirsch S, et al. Weight increase and overweight are associated with DNA oxidative damage in skeletal muscle. *Clin Nutr.* (2006)
- McDonald JC et al. Prototyping of microfluidic devices in poly (dimethylsiloxane) using solid-object printing. *Anal Chem.* (2002)

Disclaimer

This product is for research use only and is not intended for therapeutic or diagnostic applications. Please contact a technical service representative for more information. All products of animal origin manufactured by Rockland Immunochemicals are derived from starting materials of North American origin. Collection was performed in United States Department of Agriculture (USDA) inspected facilities and all materials have been inspected and certified to be free of disease and suitable for exportation. All properties listed are typical characteristics and are not specifications. All suggestions and data are offered in good faith but without guarantee as conditions and methods of use of our products are beyond our control. All claims must be made within 30 days following the date of delivery. The prospective user must determine the suitability of our materials before adopting them on a commercial scale. Suggested uses of our products are not recommendations to use our products in violation of any patent or as a license under any patent of Rockland Immunochemicals, Inc. If you require a commercial license to use this material and do not have one, then return this material, unopened to: Rockland Inc., P.O. BOX 5199, Limerick, Pennsylvania, USA.